Thermal-driven domain and cargo transport in lipid membranes

Emma L. Talbot[a], Lucia Parolini[a], Jurij Kotar[a], Lorenzo Di Michele[a], and Pietro Cicuta[a,1]

[a]Department of Physics, Cavendish Laboratory, University of Cambridge, Cambridge CB3 0HE, United Kingdom

Edited by Monica Olvera de la Cruz, Northwestern University, Evanston, IL, and approved December 13, 2016 (received for review August 13, 2016)

Domain migration is observed on the surface of ternary giant unilamellar vesicles held in a temperature gradient in conditions where they exhibit coexistence of two liquid phases. The migration localizes domains to the hot side of the vesicle, regardless of whether the domain is composed of the more ordered or disordered phase and regardless of the proximity to chamber boundaries. The distribution of domains is explored for domains that coarsen and for those held apart due to long-range repulsions. After considering several potential mechanisms for the migration, including the temperature preferences for each lipid, the favored curvature for each phase, and the thermophoretic flow around the vesicle, we show that observations are consistent with the general process of minimizing the system's line tension energy, because of the lowering of line interface energy closer to mixing. DNA strands, attached to the lipid bilayer with cholesterol anchors, act as an exemplar "cargo," demonstrating that the directed motion of domains toward higher temperatures provides a route to relocate species that preferentially reside in the domains.

vesicles | thermophoresis | DNA | lipid bilayers | lipid phase separation

Giant unilamellar vesicles (GUVs) provide a simplified model for studying various aspects of biological membranes. GUVs of a saturated lipid, an unsaturated lipid, and a sterol can form domains of coexisting liquid phases below a critical transition temperature, T_t. Domains diffuse on the surface of the vesicle with a diffusion coefficient that depends on the domain size and the membrane viscosity (1). The domain morphology is strongly linked to the temperature and composition of the membrane (2–4) and also the membrane tension (5). GUVs have been observed to form a range of shapes (6–9) and domain morphologies (2, 10), including modulated phases (11). However, to minimize their edge length, liquid phase domains most commonly form circular patches and coarsen to reduce the overall line energy over the membrane. "Normal" coarsening can occur by collision and coalescence of domains because of their diffusive motion (12, 13) or by Ostwald ripening (14). In practice, membrane curvature adds other degrees of freedom and provides another route to minimize the free energy via domain budding (15–17). Domains of the phase with a lower bending modulus may dimple from the surface of the vesicle. Repulsive interactions (associated with curvature of the membrane between domains) keep dimpled domains apart and cause a reduction in the rate of coalescence ("hindered" coarsening) (13, 18).

The behavior of domains in liquid-ordered (L_o)/liquid-disordered (L_d) phase coexistence has been explored in equilibrium and during coarsening (12). Such studies include the fluctuations in the domain boundary observed near T_t (19) and the dependence of T_t on the membrane composition (4). However, these studies look only at a fixed temperature across a domain. Although osmotic gradients have been explored to induce shape changes in vesicles (9), temperature gradients have received little attention.

In this work, we observe the behavior of domains in a thermal gradient to visualize the effect on transport processes. Domains migrate toward the hot side of a GUV for both normal and hindered coarsening regimes, regardless of their phase (L_d or L_o). The lateral transport of domains along a membrane provides a route for tailoring the membrane composition by delivery/removal of the lipids forming these domains. Similarly, species that preferentially locate within the domains [for example, some integral membrane proteins prefer to reside in cholesterol-rich regions (20)] can be moved selectively to heated regions. We use the transport of DNA constructs with cholesterol anchors, which preferentially locate in the cholesterol-rich L_o phase (21), to demonstrate this thermal manipulation mechanism.

Results and Discussion

Domain Migration on the Surface of a Vesicle. To explore the migration of domains on the surface of a vesicle, we used fluorescence microscopy to image GUVs composed of diphytanoylphosphatidylcholine (DiPhyPC)/dipalmitoylphosphatidylcholine (DPPC)/cholestanol (chol). The inclusion of a fluorescent lipid (which partitions preferentially into the L_d phase) allows us to distinguish between bright domains rich in DiPhyPC and dark domains rich in chol and DPPC. A custom-made imaging cell is used to produce a temperature gradient across a GUV. The temperature is first increased above the transition temperature, T_t, and held for 5 min to ensure that the lipids are fully mixed. The temperature is then quenched below T_t, and domain formation and migration is observed with (or without) a temperature gradient ΔT_v across the vesicle. A small density mismatch between an inner solution of sucrose and outer solution of glucose is set, to cause vesicles to sink to the cold plate and facilitate imaging. Following quenching of the sample from above the transition temperature, domains form on the surface of a vesicle. If no temperature gradient is applied, the domains coalesce over time, to form a phase-separated vesicle with one bright side (L_d) and

Significance

Giant phospholipid and sterol vesicles can separate into coexisting phase domains, observable by fluorescence microscopy. The morphology and motility of these domains provides a simplified model for processes in the plasma membrane of cells. Previous studies maintained a uniform temperature across a vesicle and showed that the morphology of the domains depends on the membrane composition and temperature. We observed the nonequilibrium behavior of domains due to a temperature gradient, revealing domain migration toward higher temperatures. This motion provides a method for controlling the localization of each phase. Species that associate with the sterol-rich regions, such as DNA constructs, can also be actively transported on the vesicle surface, allowing control over the distribution and confinement of that species via vesicle morphology.

Author contributions: P.C. designed research; E.L.T., L.P., and J.K. performed research; L.D.M. contributed new reagents/analytic tools; E.L.T. analyzed data; and E.L.T., L.D.M., and P.C. wrote the paper.

The authors declare no conflict of interest.

This article is a PNAS Direct Submission.

Data deposition: A complete dataset is available for download at https://doi.org/10.17863/CAM.6589.

[1]To whom correspondence should be addressed. Email: pc245@cam.ac.uk.

one dark side (L_o). The orientation of the L_d and L_o phases with respect to the vertical direction is random.

When a vertical temperature gradient is applied across the vesicle, the domains migrate from the cold side around to the hot cap (Fig. 1*A*). Fig. 1*B* shows an example of the L_d phase forming the domains. Crowding of the domains on the hot cap results in larger domains because of coalescence, which usually eventually merge to form one large domain on the hot side. The migration also occurs in some vesicles where the coarsening is hindered due to curvature-mediated domain repulsion (22, 23). The cold side is thus in all cases depleted of domains. Fig. 1*C* demonstrates quantitatively the increase in the area fraction of white domains (A_w/A_v) on the hot cap, and depletion on the cold cap, due to domain migration. The number of domains on the cold cap decreases due to the migration; there is also a decrease on the hot cap, due to coalescence forming fewer larger domains. The domain migration aligns the L_d and L_o phases in the fully separated vesicle with the temperature gradient (i.e., with the z direction). Note that if $T_h \geq T_t$, domains "disappear" as they enter the one phase region [$T_t \simeq 38°C$ for DiPhyPC/DPPC/chol in the ratio 27.5:27.5:45 mol% (4)]. In contrast, A_w/A_v remains constant for a vesicle with $\Delta T = 0$, as domains coalesce at a similar rate on each cap and do not migrate.

The crowding of domains is easier to observe in vesicles with hindered domains (Fig. 2*A*), as the coalescence rate is significantly reduced (13, 22, 23). Fig. 2 *B* and *C* shows the closer packing of domains on the hot cap, whereas domains on the cold side are more spread out and are relatively fewer in number. The migration is enhanced when a larger temperature difference is applied across the vesicle, which results in an increase in the area fraction of the L_d phase (which forms the circular domains in this case) on the hot side and a decrease on the cold side at larger ΔT (Fig. 2*D*). The hindered coarsening also shows that the migration is not linked to differences in coalescence or coalescence rates on the hot cap compared with the cold cap.

The crowding of domains in the hindered case is reversible (Fig. 3). Reducing the temperature gradient (or removing it altogether) allows the domains that were previously crowded onto the hot side to migrate back to the cold side (Fig. 3, $t = 20$ min). Reapplying the temperature gradient returns domains to a more clustered arrangement on the hot side of the vesicle (Fig. 3, $t =$ 40 min). However, at large ΔT_v, the barrier to coalescence is exceeded (Fig. 3, $t = 50$ min).

Migration of Species Carried Within Domains. In this section, we explore the potential for relocating a species associated with the domains of a ternary GUV. DNA constructs with two cholesterol anchors are one such species and preferentially associate with the cholesterol-rich L_o phase domains of a vesicle (21) (Fig. 1 *D* and *E*). The cholesterol anchors partition into the membrane (Fig. 1*F*), and the attached DNA is mobile across the surface of the vesicle (along with its anchor). The degree of partitioning of the DNA constructs depends on the cholesterol content of each phase and is therefore linked to both the vesicle composition and the temperature.

By combining the migration of domains in a temperature gradient with the association of DNA constructs with those domains, we show that the DNA constructs can be redistributed on the surface of the vesicle. If the circular domains are formed from the cholesterol-rich L_o phase, then the DNA constructs associate with the domains and migrate toward the hot cap of the GUV (Fig. 4 *Left*). However, if the composition of the vesicle is such that the circular domains are formed from the cholesterol-poor L_d phase, then the majority of DNA constructs are left behind on the cold side of the vesicle as the L_d domains migrate to the hot cap (Fig. 4 *Right*). Hence, by tailoring the composition of the vesicle, the species associated with the L_o phase can be directed toward high or low temperatures along a thermal gradient. DNA constructs have the added potential for modification and/or attachment.

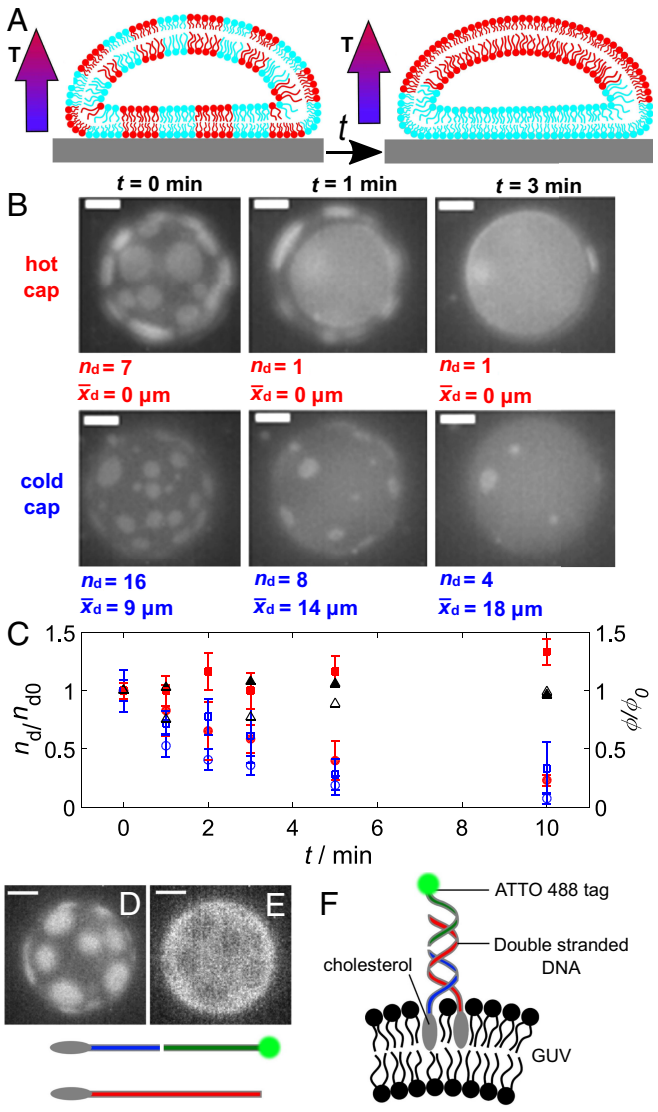

Fig. 1. Lipid domains migrate to the hot cap of a GUV in a temperature gradient and can carry associated cholesterol-anchored DNA constructs. (*A*) Schematic side view of the process of domain migration and coalescence. Coalescence increases the size of domains crowded on the hot cap to form one large domain, aligned with the temperature gradient. (*B*) Migration affects domains over all of the GUV; shown here are the hot and cold caps of the same GUV at three time points. $\Delta T_v = 2.1$ K across the vesicle. The domain number, n_d, and mean separation of nearest neighbors (center to center), $\bar{x}_d$, are shown for each cap. (*C*) Mean n_d (○) normalized by initial domain number, n_{d0}, and area fraction of white L_d domains to vesicle area, ϕ (□), normalized by the initial fraction ϕ_0 with respect to time for the cold caps (open, blue) and hot caps (closed, red). Data are in excess of 50 vesicles. Error bars are SEs on the mean. For comparison (△; closed for the hot side and open for the cold side), the area fractions of L_d domains for a vesicle with $\Delta T = 0$. (*D* and *E*) Images show 1,2-dihexadecanoyl-sn-glycero-3-phosphoethanolamine, triethylammonium salt (TX-DHPE) partitioning into the L_d phase (the circular domains, in this case) (*D*) and DNA-rich L_o regions (*E*). (*F*) Schematic of DNA construct anchored to the bilayer. Constructs are assembled from three single-stranded sequences (indicated by red, green, and blue). (Scale bars: 10 μm.)

Domain Migration Mechanisms. In this section, we discuss potential mechanisms for the migration. The first possible mechanism relies on the preference of one lipid species for the hot side over

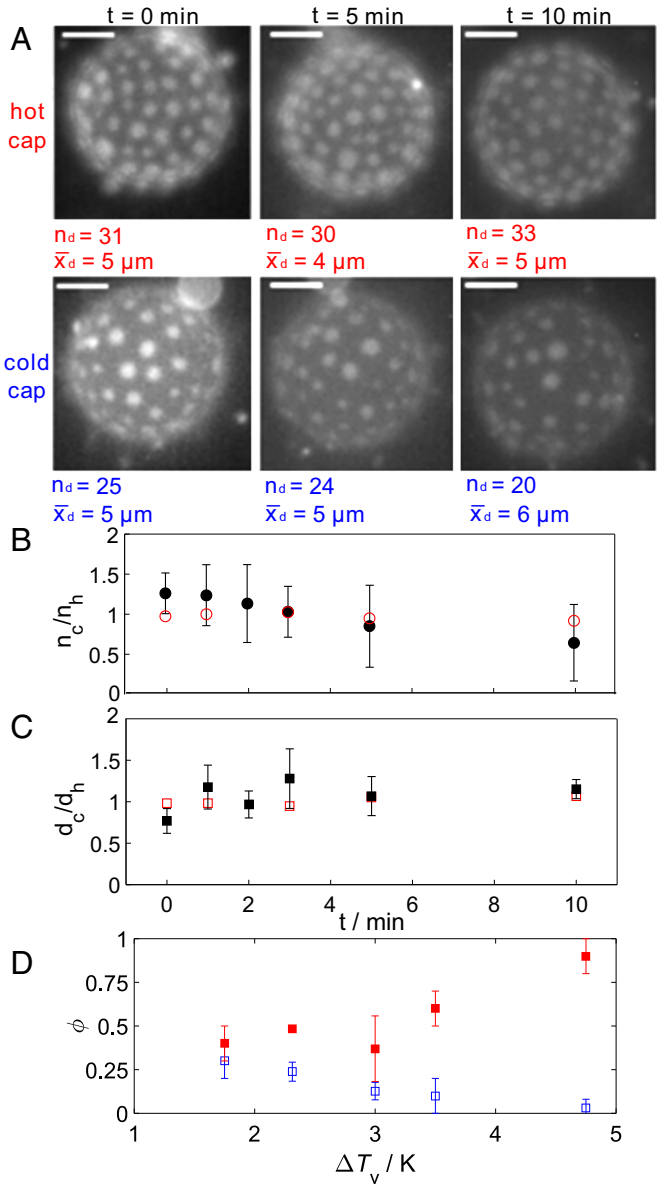

Fig. 2. Domain spacing can be controlled on a GUV with hindered coarsening. Here, membrane-mediated long-range repulsions greatly reduce the coalescence rate. Migration increases the number of domains, n_d, on the hot cap relative to the cold and increases the mean separation of nearest neighbor domains (center to center), $\bar{x}_d$, on the cold cap. (*A*) Domains on the hot and cold caps of the same GUV with time. (Scale bars: 10 μm.) ΔT_v = 1.4 K. (*B*) Mean number of domains on the cold side, n_c, normalized by the number on the hot side, n_h, with time (closed). (*C*) Mean domain spacing on the cold side, d_c, normalized by the spacing on the hot side, d_h (■). Data are in excess of 10 vesicles. Also shown is an example vesicle with $\Delta T = 0$ (□). Error bars are SEs on the mean. (*D*) Mean area fraction of white domains (■ at hot; □ at cold), relative to total vesicle area, 10 min after initialization of the temperature gradient.

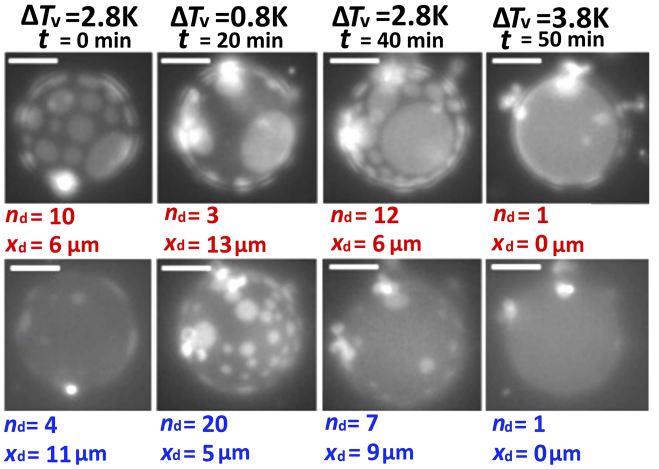

Fig. 3. Domain migration on a GUV with hindered domains is reversible. For larger ΔT_v, domains are depleted from the cold cap. Once ΔT_v is decreased, domains move back onto the cold cap (t = 20 min). The cold plate was held at 285 K and ΔT_v decreased then increased. Reapplying the temperature gradient returned domains to a crowded state on the hot cap (t = 40 min). For ΔT = 3.8 K, the barrier to coalescence was exceeded (t = 50 min). (Scale bars: 10 μm.) The number of domains, n_d, and the mean separation of nearest neighbor domains (center to center), $\bar{x}_d$, are indicated for each cap of the same GUV.

the other lipid, then that lipid would migrate toward higher temperatures. We have already noted that domains formed from the L_d phase (i.e., predominantly DiPhyPC) migrate toward the hot cap (e.g., Fig. 1). To determine whether there is a preference of DiPhyPC for the hot side, we observed domain migration on a vesicle where the domains were instead composed of the L_o phase (i.e., predominantly DPPC). Fig. 5 shows that the L_o domains also migrate to the hot side, indicating that there is no thermal preference for one lipid over the other. Domains always migrate toward the higher temperature, independent of their composition.

The second potential migration mechanism is the preference of one of the phases for regions of higher/lower curvature. The mismatch in the density of the sugar solutions inside and outside of the vesicle causes the vesicle to rest on the lower (cold) plate (see *Materials and Methods*). The solid surface causes deformation, resulting in a curvature difference between the hot and cold sides of the vesicle (as illustrated in the Fig. 1*A* schematic). Previously, L_d domains have shown a preference for regions of higher curvature (24). For GUVs resting on the lower cold plate, L_d domain migration was toward the hotter side, which had a higher curvature because it was not compressed flat by the substrate. To ensure that the migration was to regions of higher temperature and not higher curvature, the density mismatch of the sugar solution inside and outside the vesicle was reversed: GUVs now rise to the hot plate and are compressed on their hot side. Domain migration remained in the direction of the higher temperature, and hence migration was independent of the vesicle curvature, or other terms of affinity for the imaging chamber window.

The third potential mechanism is the difference in the line tension across a domain because of the temperature gradient across the vesicle. Migration toward hotter temperatures provides a route to minimize the line interface energy of the domains. The line tension, λ, of DiPhyPC/DPPC/chol vesicles decreases linearly over a range of at least 10°C, with increasing temperature close to T_t (19), and hence $\Delta\lambda$ across the domain does not depend on the absolute temperature. There is, however, an effective force due to translating the domain interface toward higher temperature (closer to mixing) because this lowers the line interface energy, E. The magnitude of the force due to translating a domain of radius r along the thermal gradient in the z direction is

$$F_t = \frac{\partial E}{\partial z} = \frac{2\pi r \partial \lambda}{\partial z}. \quad [1]$$

This force is resisted by the drag force, F, and results in a drift velocity

$$v = \frac{F}{\zeta}, \quad [2]$$

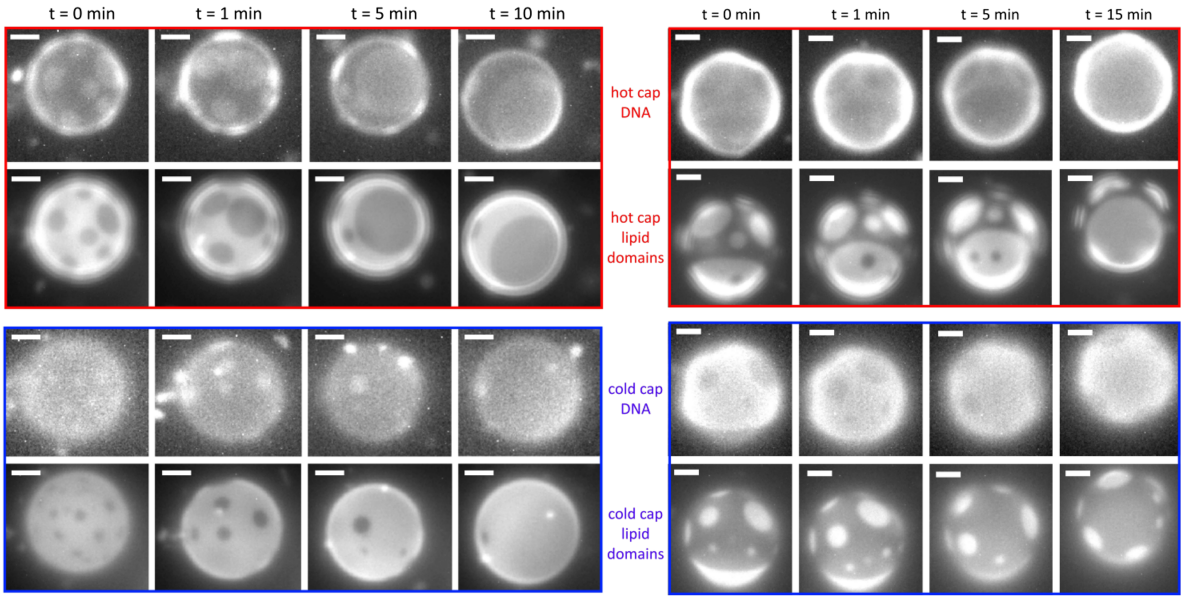

Fig. 4. Domains and DNA constructs are colocalized and transported in the temperature gradient. Images show hot and cold caps of the same GUV (*Left*, DiPhyPC/DPPC/chol 23:47:30 mol%; *Right*, DiPhyPC/DPPC/chol 1:1:1 mol%). DNA constructs partition preferentially into the L_o phase. (*Left*) L_o circular domains migrate toward higher temperatures, depleting the cold cap and leaving it rich in the L_d phase. DNA constructs are transported with the L_o domains to enrich the hot cap of the GUV. (*Right*) DNA cargo is left behind on the cold cap as L_d domains migrate to the hot cap (Scale bars: 10 μm.) ΔT_v = 2.3 K (*Left*) and 2.6 K (*Right*).

where ζ is the drag coefficient, in general related to the diffusion coefficient of a domain, D, by

$$\zeta = \frac{k_B T}{D}, \quad [3]$$

where k_B is the Boltzmann constant and T is the absolute temperature.

The form of the drag coefficient is dependent on the domain size (1, 25). For small domains ($r < \eta''/\eta_w$), the drag coefficient has the Saffman–Delbruck form and is also dependent on the membrane viscosity:

$$\zeta(r) = \frac{4\pi\eta''}{\left[ln\left(\frac{\eta''}{\eta_w}\frac{1}{r}\right) - \gamma + \frac{1}{2}\right]}, \quad [4]$$

where η'' is the 2D membrane viscosity [$\simeq 10^{-8}$ N s m^{-1} (1)], η_w is the 3D bulk viscosity (of water, $\simeq 10^{-3}$ Pa s), and γ=0.5772 is Euler's constant. For larger domains ($r > \eta''/\eta_w$, $\sim r > 10$ μm in this case), the drag coefficient is independent of the membrane viscosity,

$$\zeta(r) = 16\eta_w r. \quad [5]$$

In our case, we consider only domains with $r < 10$ μm, and therefore use Eq. **4** for our calculations.

Let us estimate the drift velocity of a domain of 5 μm diameter. The temperature gradient is $\partial T/\partial z = 0.1$ K μm^{-1}. The change in line tension with temperature is $d\lambda/dT = 0.1$ pN K^{-1}. Thus, considering the domain perimeter, following the argument above, the force is 0.15 pN. The drag coefficient of domains on the cold side of a 30 μm diameter GUV ($T = 299$ K, $\Delta T_v \simeq 3$ K) can thus be estimated $\zeta \simeq 9 \times 10^{-8}$ N s m^{-1} for domains with a radius of 2.5 μm using Eq. **4**. Therefore, the corresponding drift velocity (from Eq. **2**) is 1.5 μm s^{-1}. This number can be compared with the experimentally observed drift, keeping in mind that this estimate is only expected to hold as an order of magnitude because of (*i*) the uncertainty on the precise value of membrane viscosity (and its change across the vesicle) and (*ii*) the fact that we do not observe domain displacements purely along the temperature gradient axis. Tracking approximately 20 domains of mean radius $r \simeq 2.5$ μm on the surface of a 30 μm GUV provides a measure of the domain drift velocity of $v \simeq 0.4$ μm s^{-1} for $\Delta T_v \simeq 3$ K. This estimate is of the same order as what we estimated from the line tension argument and suggests that this is indeed the mechanism for the migration of domains toward the hot cap of a vesicle. A further corroboration comes from comparing measurements of the mean squared displacement (msd) of domains with/without an applied temperature gradient. When no thermal gradient is applied, domains follow diffusive motion (Fig. 6).

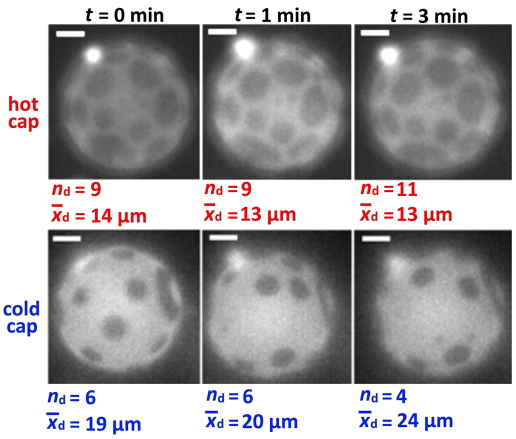

Fig. 5. Domain migration to the hot cap is independent of lipid species. Circular domains of the L_o phase also migrate toward the hot cap, indicating that there is no preference of one lipid over the other for the hot side. Domains in a GUV with hindered coarsening are shown on the hot and cold caps; time is measured from the quench below T_t (ΔT_v = 1.4 K). (Scale bars: 10 μm.) The number of domains, n_d, increases on the hot cap, and the mean center-to-center distance of nearest neighbor domains, $\bar{x}_d$, decreases relative to the cold cap.

However, on applying a thermal gradient, domains begin to move with a drift velocity (dependent on the domain radius and temperature) toward the hot side of the GUV. This drift velocity is predicted well by the line tension mechanism using Eqs. **1–4** (Fig. 6*B*).

The membrane viscosity has a strong temperature dependence, decreasing at higher temperatures (1), which would in turn progressively lower the drag coefficient (and thus increase the msd) of domains migrating to the hot side. This could contribute to a higher-than-linear dependence of the msd on time, as the domain moves to hot, but does not seem to us sufficient to explain the driven migration, and neither the magnitude of the observed msd: for a domain radius = 1.25 μm, with a temperature on the cold cap of 288 K and on the hot cap of 291 K, membrane viscosity $\simeq 2\times10^{-8}$ N s m^{-1} at 291 K, then based on diffusion the msd (80 s) $\simeq 7\,\mu m^2$. This msd (80 s) is lower than the observed msd in the thermal gradient ($\simeq 15\ \mu m^2$), which we attribute to thermal drift.

It is worth noting that the variation in line tension with temperature is dependent on the chain length of the saturated lipid. In addition, the chain length of the saturated lipid influences the membrane viscosity. For small domain sizes ($r < \eta''/\eta_w$), the drag coefficient is dependent on the membrane viscosity, and as such the chain length of the lipid will also influence the drift velocity in this manner.

An additional mechanism to consider is that the temperature-dependent interactions between the GUV and the surrounding solvent could generate a thermophoretic flow field around the vesicle (26). For a thermophobic vesicle, the flow across the surface of the vesicle is toward the hot cap. We explore whether the magnitude of this flow is significant enough to drag domains on the surface of the vesicle toward the hot side. Note that a thermal Marangoni flow in the membrane would be directed toward colder regions, where the surface tension would be higher, and as such it is not a viable mechanism for domain migration to the hot cap. For large particles, the thermophoretic force can be approximated as in ref. 26, by

$$F_T = -S_T T k_B \nabla T, \qquad [6]$$

where S_T is the Soret coefficient. In response to the thermophoretic force, an equal opposite reaction in the surrounding solvent generates a flow around the surface of the vesicle. Balancing F_T against Stokes' drag allows an estimate of the velocity in the z-direction to be calculated, from

$$v_z = -\frac{S_T T k_B \nabla T}{6\pi\eta_w a}, \qquad [7]$$

where a is the radius of the vesicle.

A proportionality relationship has been established between the radius of a particle, a, and the magnitude of the Soret coefficient, S_T, for polystyrene beads (27). On the basis of this relationship, a polystyrene bead with $a = 15\,\mu$m, has $S_T \simeq 90$ K^{-1}. We have found the Soret coefficients of 1 μm vesicles to be an order of magnitude less than polystyrene particles of the same size and therefore use an upper estimate of the Soret coefficient for vesicles ($a = 15\,\mu$m) of 9 K^{-1}. For a temperature gradient of 0.1 K μm^{-1}, an upper estimate of the velocity on the cold side of the vesicle ($T = 299$ K) is $v_z \simeq 0.01\ \mu m\ s^{-1}$, which corresponds to a thermophoretic force of $F_T \simeq 4\times10^{-3}$ pN. This velocity is much smaller than the observed drift velocity of the domains (Fig. 6*B*). Furthermore, the drift velocity varies linearly with the temperature difference across a domain.

Last, an observation: The noninterface (bulk) parts of the vesicle membrane coexist at different temperatures. To get a sense of what this implies requires thinking of a specific model for the bulk free energy, e.g., a regular solution theory for a binary mixture. If one thinks of a "regular solution" binary mixture and assumes the enthalpic term to be athermal, then it can be shown that the bulk free energies are temperature dependent. However, for each "parcel" of membrane of one phase that migrates from hot to cold, there is one of the other phase that goes the other way. Each of these parcels equilibrates concentrations (following temperature equilibration) with its new surroundings. So, for a perfectly symmetric free energy functional, like the one of a regular binary mixture, the changes in bulk free energy of the two parcels will exactly cancel out in the swap, and the net bulk free energy change would be zero. If the bulk free energy functional were substantially asymmetric, then one specific phase would prefer the hot, and the other the cold. However, this is not compatible with the experimental observation that the small domains are systematically driven toward the hot, regardless of their phase.

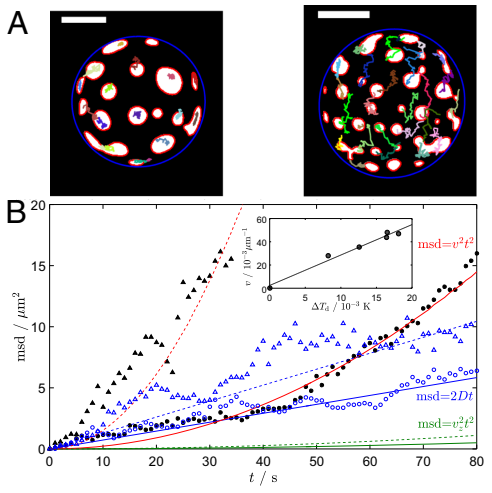

Fig. 6. Domains drift in a thermal gradient toward the hot cap, and follow diffusive motion for $\Delta T = 0$. (*A*) Domain tracks for a typical GUV (temperature cold side, $T_c = 288\,K$) with $\Delta T = 0$ (diffusive motion only) and $\Delta T = 15K$ (combined diffusive and directed motion) over a 40-s period, superposed to initial positions of domains (segmented, in white) on the cold side of a GUV (diameter ∼30 μm). The blue circle indicates the GUV perimeter, and red lines show domain boundaries. (Scale bars: 10 μm.) (*B*) msd for $\Delta T = 0$ (blue data, solid fits) and ΔT = 15 K (black data, dashed fits) at T_c = 288 K (○) and T_c = 299 K (△). Curves show msd assuming diffusive motion with the Saffman–Delbruck form of the drag coefficient (blue); thermal drift driven by the variation in line tension across a domain (red); and a thermophoretic mechanism (green). *B*, *Inset* shows the linearity of drift velocity, *v*, against temperature difference across a domain, ΔT_d (mean domain radius 1.25 μm and mean GUV radius 14 μm).

Conclusion

When a temperature gradient is applied across a GUV, domains migrate across the surface of the vesicle toward higher temperatures. Migration occurs independent of whether the domains are formed predominantly from the liquid-ordered or -disordered phase. For vesicles that experience normal coarsening, the domains migrate toward the side of the vesicle at a higher temperature because of the mismatch in line tension across a domain. By moving toward hotter temperatures, the domains minimize their line interface energy. The domains also coalesce, resulting in a phase-separated vesicle with a single liquid-ordered domain and a single liquid-disordered domain aligned with the direction of the temperature gradient. For hindered coarsening regimes, the domain coalescence rate is slowed. In this case, the domain spacing may be reversibly altered by applying or removing the temperature gradient. Domains on the cold side are further apart than on the hot side when the thermal gradient is applied.

By including a species that preferentially associates with the domains of a ternary GUV, that species can be selectively

moved and even localized on the surface of a vesicle. DNA constructs with cholesterol anchors preferentially locate within the cholesterol-rich L_o phase. Domain migration relocates the DNA constructs to the cold side of the vesicle if domains are the L_d phase. If the L_d and L_o phases are switched, then the DNA constructs (which are now associated with the L_o domains) instead locate to the hot side of the vesicle. DNA constructs provide an easy route for modification or attachment of other species, which could then be distributed over the vesicle. The same principle could be applied to proteins that have a composition preference. Similarly, local heating of a supported bilayer with mobile domains could enable directed motion of species associated with the domains.

Materials and Methods

Ternary GUVs. Vesicles were prepared via electroformation (28, 29) from DPPC (chain melting temperature 41°C), DiPhyPC (chain melting temperature <-120°C), and cholestanol (chol). Lipids were purchased from Avanti Polar Lipids in chloroform and used in the molar ratio 27.5:27.5:45 (DPPC:DiPhyPC:chol). Chol (Sigma-Aldrich) was used in place of cholesterol to reduce photooxidation. A fluorescent lipid labeled with Texas Red dye, 1,2-dihexadecanoyl-sn-glycero-3-phosphoethanolamine, triethylammonium salt (TX-DHPE), was purchased from Invitrogen and included at 0.8 mol%. The fluorescent lipid partitions preferentially into the L_d phase. GUVs were prepared to include an inner solution of 197 mM sucrose (Sigma-Aldrich) and an outer solution of 200 mM glucose (Sigma-Aldrich) to ensure that the vesicles rested on the bottom surface.

DNA Constructs. Cholesterol anchors on DNA constructs provide a hydrophobic modification sufficient to allow spontaneous insertion into the bilayer. Such constructs show a compositional preference when associating with the phase domains of a vesicle. The constructs are self-assembled from the following single-stranded DNA sequences: 5′-CGTGCGCTGGCGTCTGAAA-GTCGATTGCGAAAA-3′-cholesterol-TEG (Integrated DNA Technologies), Cholesteryl-TEG-5′-TTTTCGCAATCGACTTT-3′ (Eurogentec), and 5′-CAGACGC-CAGCGCACGAAA-3′-ATTO488 (Integrated DNA Technologies). Single-stranded DNA sequences were purchased, lyophilized, reconstituted in TE buffer [10 mM Tris(hydroxymethyl)aminomethane and 1 mM ethylenediaminetetra acetic acid; Sigma-Aldrich], and mixed in stoichiometric ratio in TE buffer with 100 mM NaCl. The mixture was heated to 90°C and cooled slowly to enable the self-assembly of the DNA construct shown in Fig. 1*F*. The ATTO488 dye enables fluorescence microscopy of the DNA constructs. GUVs containing 300 mM sucrose were prepared via electroformation (to ensure vesicles were denser than the surrounding solution) and were functionalized by mixing 2 μL of the GUV sample with 90 μL iso-osmolar TE buffer solution containing 87 mM glucose, 100 mM NaCl, and DNA constructs. The final concentration of DNA constructs was 0.15 μM. DNA-coated vesicles were left under rotation at room temperature overnight to enable DNA binding. The solution was then removed from rotation, and vesicles were allowed to sink for 5–10 min before a sample of 30 μL was extracted from the bottom of the vial for use in the experiments. Further details on the DNA preparation and vesicle coating can be found in ref. 30.

Imaging. A custom-made imaging cell was prepared consisting of a 200 μm thick silicone spacer (possessing a hole to contain the vesicle suspension), sandwiched between two sapphire windows. The windows were placed on a cooled metal plate connected to a water bath and held on top by a heated metal plate. A central hole was cut into the plates to enable imaging of the vesicles. Thermocouples were used to measure the temperature of the plates. The temperature of the hot plate, T_h, was held fixed by using a custom-built temperature controller with a feedback loop. The applied linear temperature gradient (ΔT) was vertical, with a hotter upper surface, to avoid convection. For imaging DNA-coated vesicles, bovine serum albumin (Sigma-Aldrich; rehydrated in water to form a 1% solution) was used to passivate glass cover slips, which were "stuck" to the sapphire windows with a little water so that the DNA/vesicle suspension was not directly in contact with the sapphire.

Fluorescence imaging of the vesicles was carried out by using a Nikon Eclipse Ti-E inverted microscope equipped with a 40× objective lens (Nikon; S Plan Fluor, ELWD 2.8–3.6 mm, NA 0.6) and a camera (Point Gray Research; Grasshopper3 GS3-U3-23S6M). Samples were illuminated with either a metal halide lamp or a single-color LED through a Texas Red filter set (Semrock; exciter FF01-562/40, dichroic FF593-Di02, emitter FF01-624/40). A z stack was taken across the vesicle, and the slices were analyzed by using custom-made MATLAB image analysis routines. The slice showing the domains on the top side is referred to as the hot cap, and the bottom side as the cold cap. For DNA-coated vesicles, the DNA was imaged by using a GFP filter set (Semrock; exciter FF01-472/30, dichroic FF495-Di03, emitter FF01-520/35).

ACKNOWLEDGMENTS. This work was supported by Engineering and Physical Sciences Research Council (EPSRC) GrantEP/J017566/1. L.D.M. was supported by the Oppenheimer Fund, Emmanuel College Cambridge, Leverhulme Trust, and Isaac Newton Trust through an Early Career Fellowship.

1. Cicuta P, Keller SL, Veatch SL (2007) Diffusion of liquid domains in lipid bilayer membranes. *J Phys Chem B* 111:3328–3331.
2. Veatch SL, Keller SL (2003) Separation of liquid phases in giant vesicles of ternary mixtures of phospholipids and cholesterol. *Biophys J* 85:3074–3083.
3. Veatch SL, Keller SL (2005) Seeing spots: Complex phase behavior in simple membranes. *Biochim Biophys Acta* 1746:172–185.
4. Veatch SL, Gawrisch K, Keller SL (2006) Closed-loop miscibility gap and quantitative tie-lines in ternary membranes containing diphytanoyl PC. *Biophys J* 90:4428–4436.
5. Chen D, Santore MM (2014) Large effect of membrane tension on the fluid-solid phase transitions of two-component phosphatidylcholine vesicles. *Proc Natl Acad Sci USA* 111:179–184.
6. Baumgart T, Hess ST, Webb WW (2003) Imaging coexisting fluid domains in biomembrane models coupling curvature and line tension. *Nature* 425:821–824.
7. Yu Y, Granick S (2009) Pearling of lipid vesicles induced by nanoparticles. *J Am Chem Soc* 131:14158–14159.
8. Yoon YZ, Hale JP, Petrov PG, Cicuta P (2010) Mechanical properties of ternary lipid membranes near a liquid-liquid phase separation boundary. *J Phys Condens Matter* 22:062101.
9. Tomita T, Sugawara T, Wakamoto Y (2011) Multitude of morphological dynamics of giant multilamellar vesicles in regulated nonequilibrium environments. *Langmuir* 27:10106–10112.
10. Gutlederer E, Gruhn T, Lipowsky R (2009) Polymorphism of vesicles with multi-domain patterns. *Soft Matter* 5:3303–3311.
11. Amazon JJ, Goh SL, Feigenson GW (2013) Competition between line tension and curvature stabilizes modulated phase patterns on the surface of giant unilamellar vesicles: A simulation study. *Phys Rev E* 87:022708.
12. Stanich CA, et al. (2013) Coarsening dynamics of domains in lipid membranes. *Biophys J* 105:444–454.
13. Yanagisawa M, Imai M, Masui T, Komura S, Ohta T (2007) Growth dynamics of domains in ternary fluid vesicles. *Biophys J* 92:115–125.
14. Lifshitz IM, Slyozov VV (1961) The kinetics of precipitation from supersaturated solid solutions. *J Phys Chem Solids* 19:35–50.
15. Lipowsky R (1992) Budding of membranes induced by intramembrane domains. *J Phys II* 2:1825–1840.
16. Lipowsky R (1993) Domain-induced budding of fluid membranes. *Biophys J* 64:1133–1138.
17. Lipowsky R, Dimova R (2003) Domains in membranes and vesicles. *J Phys Condens Matter* 15:S31–S45.
18. Ursell TS, Klug WS, Phillips R (2009) Morphology and interaction between lipid domains. *Proc Natl Acad Sci USA* 106:13301–13306.
19. Honerkamp-Smith AR, et al. (2008) Line tensions, correlation lengths, and critical exponents in lipid membranes near critical points. *Biophys J* 95:236–246.
20. Samsonov AV, Mihalyov I, Cohen FS (2001) Characterization of cholesterol-sphingomyelin domains and their dynamics in bilayer membranes. *Biophys J* 81:1486–1500.
21. Beales PA, Vanderlick TK (2009) Partitioning of membrane-anchored DNA between coexisting lipid phases. *J Phys Chem B* 113:13678–13686.
22. Semrau S, Idema T, Schmidt T, Storm C (2009) Membrane-mediated interactions measured using membrane domains. *Biophys J* 96:4906–4915.
23. Idema T, Semrau S, Storm C, Schmidt T (2010) Membrane mediated sorting. *Phys Rev Lett* 104:198102.
24. Feriani L, Cristofolini L, Cicuta P (2015) Soft pinning of liquid domains on topographical hemispherical caps. *Chem Phys Lipids* 185:78–87.
25. Saffman PG, Delbrück M (1975) Brownian motion in biological membranes. *Proc Natl Acad Sci USA* 72:3111–3113.
26. Yang M, Ripoll M (2013) Thermophoretically induced flow field around a colloidal particle. *Soft Matter* 9:4661–4671.
27. Braibanti M, Vigolo D, Piazza R (2008) Does thermophoretic mobility depend on particle size? *Phys Rev Lett* 100:108303.
28. Angelova MI, Dimitrov DS (1986) Liposome electroformation. *Faraday Discuss Chem Soc* 81:303–311.
29. Angelova MI, Soléau S, Méléard PH, Faucon F, Bothorel P (1992) Preparation of giant vesicles by external AC fields. Kinetics and applications. *Prog Colloid Polym Sci* 89:127–131.
30. Parolini L, et al. (2015) Volume and porosity thermal regulation in lipid mesophases by coupling mobile ligands to soft membranes. *Nat Comm* 6:5948.